

Available online at [www.sciencedirect.com](http://www.sciencedirect.com)**SciVerse ScienceDirect**

Procedia Computer Science 18 (2013) 2028 – 2035

**Procedia**  
Computer Science

2013 International Conference on Computational Science

## DDDAMS-based Crowd Control via UAVs and UGVs

Zhenrui Wang<sup>a</sup>, Mingyang Li<sup>a</sup>, Amirreza M. Khaleghi<sup>a</sup>, Dong Xu<sup>a</sup>, Alfonso Lobos<sup>a</sup>,  
Christopher Vo<sup>b</sup>, Jyh-Ming Lien<sup>b</sup>, Jian Liu<sup>a</sup>, Young-Jun Son<sup>a, \*</sup>

<sup>a</sup>Systems and Industrial Engineering, The University of Arizona, Tucson, AZ 85721-0020, USA<sup>b</sup>Computer Science, George Mason University, Fairfax, VA 22030, USA

### Abstract

Unmanned aerial vehicles (UAVs) and unmanned ground vehicles (UGVs) collaboratively play central roles in intelligence gathering and control in urban/border surveillance and crowd control. In this paper, we first propose a comprehensive planning and control framework based on dynamic-data-driven, adaptive multi-scale simulation (DDDAMS). We then discuss proposed algorithms enabling DDDAMS capability based on several methods such as 1) Bayesian-based information aggregation/disaggregation, 2) dynamic information updating based on observation/simulation, 3) temporal and spatial data fusion for enhanced performance, 4) multi-resolution strategy in temporal tracking frequency, and 5) cached intelligent observers. Finally, preliminary results based on the proposed framework, algorithms, and testbeds are discussed.

© 2013 The Authors. Published by Elsevier B.V. Open access under [CC BY-NC-ND license](https://creativecommons.org/licenses/by-nc-nd/4.0/).

Selection and peer review under responsibility of the organizers of the 2013 International Conference on Computational Science

*Keywords:* Crowd control; UAV; UGV; multi-scale; agent-based simulation

### 1. Introduction

Unmanned aerial vehicles (UAVs) and unmanned ground vehicles (UGVs) collaboratively play central roles in information gathering and control in border/urban surveillance and crowd control. Scalable, robust, and effective monitoring, tracking, and control of crowd is challenging as the considered systems are highly complex, dynamic, and uncertain, involving human behaviors, numerous autonomous hardware and software technologies, and environmental conditions. The goal of our long-term research is to investigate algorithmic approaches to create scalable, robust, multi-scale, and effective urban surveillance and crowd control strategies using UAVs and UGVs. Scalability will provide group control over behavior-rich group with hundreds to thousands of group members. Robustness will allow the controller agents (UAVs and UGVs) to generate

\* Corresponding author. Tel.: +1-520-626-9530; fax: +1-520-621-6555.

E-mail address: [son@sie.arizona.edu](mailto:son@sie.arizona.edu).

control strategy even when the behaviors of the controlled group are not well modeled due to many sources of inevitable uncertainty. In order to achieve our objective, we have proposed a comprehensive planning and control framework based on dynamic-data-driven, adaptive multi-scale simulation (DDDAMS), where dynamic data is incorporated into simulation, simulation steers the measurement process for data update and system control, and an appropriate level of simulation fidelity is selected based on the time constraints for evaluating alternative control policies using simulation. In our research, the DDDAMS framework that was developed by the authors for the case of extended manufacturing enterprise [1] has been leveraged to address scalable, robust, multi-scale, and effective surveillance and crowd control via UAVs and UGVs.

The particular goal of this paper is three-fold. First, the proposed DDDAMS-based planning and control framework is discussed. Second, we discuss proposed algorithms enabling DDDAMS capability, where they are based on several methods such as 1) Bayesian-based information aggregation/disaggregation among UAVs and UGVs, 2) dynamic information updating based on observation/simulation, 3) temporal and spatial data fusion for enhanced performance, 4) multi-resolution strategy in temporal tracking frequency, and 5) cached intelligent observers. Third, we discuss testbeds involving real UAVs and other virtual components.

## 2. Proposed DDDAMS-based Planning and Control Framework

### 2.1. Scenario: Surveillance and Crowd Control

In the surveillance of a crowd, UGVs and UAVs collaborate in a complementary manner to achieve detecting, tracking and control of individuals in the crowd [2]. Specifically, UAVs offer the searching capability in a wider area and a global view of the crowd. However, the accuracy of the information on target localization is restricted by various factors, such as the speed and altitude limits, on-board sensor resolution, and environmental disturbances. UGVs, on the other hand, complement UAVs' deficiency by providing accurate sensing capability. However, their observation range is often smaller than that of UAVs and may be obstructed by nearby obstacles. Fig 1 illustrates such information insufficiency if either UGVs or UAVs are deployed alone. UGVs can observe dynamic movements of individual agents in a sub-crowd within their observation range, with high resolution. UAVs can provide global but less accurate information on the overall dynamic movement of the crowd. By integrating the information from both UGVs and UAVs up to time  $t$ , the dynamics of the crowd region at future time horizon, e.g., time  $t+1$ , can be better estimated.

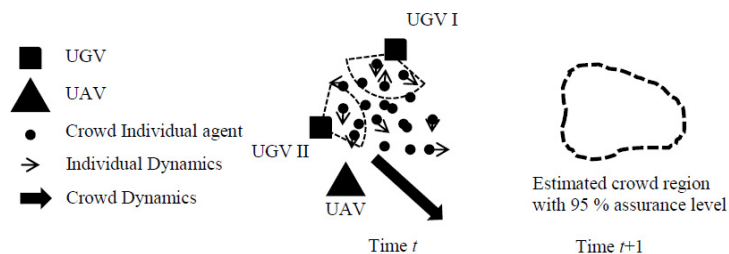


Fig. 1. Complementary role of the UGVs and UAVs

### 2.2. Overview of DDDAMS-based Planning and Control Framework

Fig 2 depicts the proposed DDDAMS-based planning and control framework, in which decision planner, controller and real system are integrated for surveillance and crowd control via UAVs and UGVs. Switching between planning and control occurs on a temporal basis or event basis. While planning is performed for equal intervals under the temporal mechanism, planning under the event-based mechanism is triggered when a

deviation between planned and observed system performances exceeds a threshold value. The system performance criteria include generic measurement of effectiveness (MOE) for UAV/UGV mission tasks, where the common ones are the probability of object detection and the duration percentage of successful tracking.

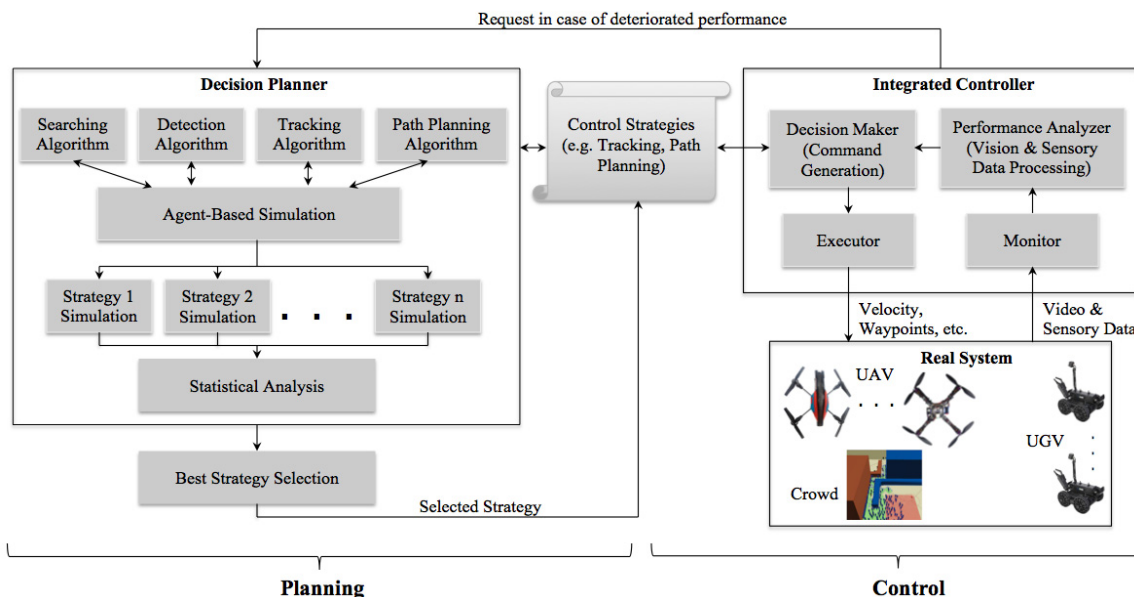


Fig. 2: DDDAMS-based planning and control framework

During the planning stage, a decision planner, which has been implemented in an agent-based simulation environment, will devise a set of best UAV/UGV control strategies for the evolution of real system. Various algorithms (e.g. UAV/UGV searching, detection, tracking, path planning) are implemented in the agent-based simulation, which helps evaluate alternative control strategies against different scenarios. For instance, UAV/UGV path planning algorithm involves selecting one from deterministic, probabilistic, and mixed strategies (to list a few). Under a similar problem setting, the results may vary according to different choices of strategy [3,4]. In addition, as different algorithms (e.g. tracking, path planning) are integrated in the same simulation environment, strategy interactions and trade-offs should be considered for achieving the best system level performance in favor of individual algorithm performance. Next, each potential strategy combination is initialized as an instance for simulation-based evaluation. At the final step, statistical analyses (e.g. confidence interval, hypothesis testing) are performed for selecting the best control strategies due to the variations inherently in the simulation outputs. In this work, the agent-based simulation models have been implemented in Repast Symphony<sup>®</sup> (see Fig 3(a)), and the statistical tool used is R<sup>®</sup>.

At the control side, an integrated controller consisting of four individual components (i.e. decision maker, executor, monitor, and performance analyzer) has been developed. The decision maker 1) utilizes the best control strategies to generate real-time commands (e.g. velocity, waypoints) for UAV/UGV operations, and 2) to invoke the decision planner when the actual system performance deviates substantially from the predicted system performance. The executor is directly linked with decision maker for receiving commands and sending them into the real system. The communication between real hardware and executor is performed using open-source micro air vehicle communication protocol called MAVLink. The monitor updates the entire system status based on feedback information (e.g. video, sensory data) from the real system, and then forwards it to the performance analyzer. An open source, cross-platform software package called QGroundControl<sup>®</sup>, has been

employed in this work, which has implemented the functionality of executor and monitor (see Fig 3(b)). Finally, the performance analyzer 1) processes the picture, video stream, and sensory data transformation and linking the transformed data with the performance criteria and 2) compares the actual and predicted system performance and calls for the decision maker if necessary. Currently, the software implementation for the performance analyzer consists of different algorithms (e.g. motion detection algorithm, motion tracking algorithm) in OpenCV<sup>®</sup> (Open Source Computer Vision). Fig 3(c) depicts the quad copter that has been developed at University of Arizona and George Mason University, which includes 5000 mAh battery, GPS, telemetry, and can handle an additional payload of 1200g for at least 25 minutes. The real UAVs with virtual components in the simulation constitute testbeds that can be used to evaluate the proposed control framework.



Fig. 3. (a) Snapshot of agent-based simulation; (b) Snapshot of QGroundControl<sup>®</sup> with waypoints; (c) UAVs available at UA and GM

### 3. Proposed Algorithms Enabling DDDAMS Capability

#### 3.1. Crowd Motion Modeling

In this research, we adopt the state vector  $\mathbf{x}_i(t)$ ,  $i=1,2,\dots,M$ , for individual agents in a crowd at time  $t$ , where  $M$  is the total number of individual agents in the crowd, as depicted in Fig 1. The state vector contains state information of an individual agent, including its preference state, such as moving speed and direction, and geographic state, such as locations. Thus the preference state vectors are used as elements to model the complex spatial/temporal problem. The state vector of a crowd at time  $t$  can be represented as a stack-up of all the  $M$  state vectors, i.e.,  $\mathbf{x}(t) = [(\mathbf{x}_1(t))^T \ (\mathbf{x}_2(t))^T \ \dots \ (\mathbf{x}_M(t))^T]^T$ . The preference and geographic states of an individual agent at time  $t+1$  are mainly affected by three types of factors: 1) the preference of crowd individuals, including itself, at time  $t$ ; 2) the environmental factors that affect crowd preferences; and 3) the impacts of the controlling units, such as UAVs and UGVs. These complex relationships can be modeled by:

$$\mathbf{x}(t+1) = \mathbf{A}(t) \cdot \mathbf{x}(t) + \mathbf{B}_f(t) \cdot \mathbf{f}(t) + \mathbf{B}_u(t) \cdot \mathbf{u}(t) + \mathbf{w}(t), \quad t=1,2,\dots, \quad (1)$$

where  $N$  is the total number of time steps;  $\mathbf{A}(t)$  represents the moving dynamics of crowd agents;  $\mathbf{B}_f(t)$  represents the impacts of the environmental factors,  $\mathbf{f}(t)$ , on agents' states;  $\mathbf{B}_u(t)$  represents the impacts of controlling activities,  $\mathbf{u}(t)$ , on agents' states;  $\mathbf{w}(t)$  represents the un-modeled errors. The state vectors of individual agents may not be directly observable due to the resolution or range deficiency of sensors. Therefore, a measurement model is often considered to represent the observation as a linear combination of true state vector and observation noise, such as the one used in Kalman filter [5].

#### 3.2. Crowd Motion Detection

Local motions necessary for the camera to maximize its visibility of the human crowd are considered. It is noted that the camera motion is to locally adjust the camera locations/directions to achieve the best

observations of the crowd. In most of the existing methods available in the literature, it is assumed that that maintaining the visibility of a single reference point (e.g., the center of mass) will provide the visibility to the entire target. However, it usually is not the case in the real world.

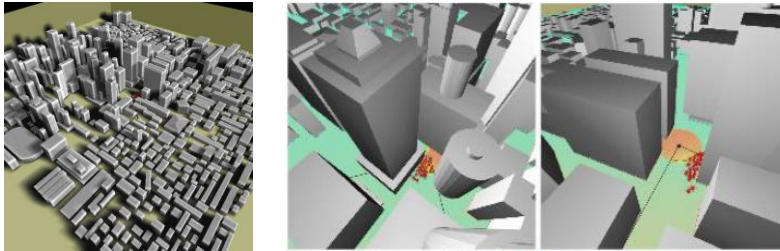


Fig 4. (a) A virtual city with 161 building; (b) Snapshots of CIOg camera following 30 targets in the city environment in (a)

Among widely known methods, the Intelligent Observer (IO) [6] camera provides a high success rate, but is extremely inefficient. The Visibility-Aware Roadmap (VAR) [7] camera provides fast online tracking strategy through the use of pre-computed visibility information, but it performs worse than IO in terms of visibility. To address this issue, we propose two camera planning methods called Cached Intelligent Observers (CIO): CIOg and CIOc [8]. These new methods provide comparable performance to both IO and VAR while reducing the offline computation and maintaining efficiency in determining camera motions online. The main idea is to incrementally build and cache the visibility information in the vicinity of the targets and the camera. These new methods can be viewed as an improved IO camera that reduces the visibility computation complexity to almost constant. The CIOg method begins by creating a two dimensional grid. For each grid point, CIOg caches a certain amount of information about not only itself (such as its distance from the nearest obstacle), but also about other grid points in the network (such as its visibility to other points). Like its predecessor, IO [6], at each time step, CIOg uses prediction and evaluation of camera and target positions to try and find an ideal location for the camera to maintain visibility of the as much of the flock as possible for the next time step. In CIOc, a slightly different approach is taken to storing visibility information in the space. First, using disc-like partitions, a graph is computed as well as a visibility graph among overlapping partitions of the workspace. As with CIOg, these data structures are used with successive cycles of prediction and evaluation of future target and camera positions to make decisions about where to move next. Fig. 4(b) shows an example of CIOg successfully following 30 targets in the city environment shown in Fig. 4(a).

### 3.3. Crowd Motion Tracking and Controlling

Based on the observation of crowd motion, the crowd tracking algorithm can be developed. Different from the camera planning algorithm, the objective of crowd tracking and controlling is to plan the moving paths of UAVs and UGVs to follow and affect the crowd motion. This is achieved by predicting the location of individual agents at next time step, based on the current observation achieved by CIOs. Various tracking algorithms have been proposed in the literature, such as Kalman filter [5] and its extension [9], grid-based tracking [10,11], and particle filter [12]. This paper adopts the Kalman filter for tracking of individual agents, since Kalman filter has been proved to be optimal for linear dynamic systems with Gaussian noises, which is often mathematically formulated with the state space model similar to Eq. (1).

Information collected from both UAVs and UGVs should be utilized together to capture the dynamic characteristic of the overall crowd. The high resolution observations on sub-crowd or individuals collected by UGVs should be aggregated to be combined with UAVs' direct observations of the overall crowd dynamics. Denote the parameter set  $\Theta_t = \{\mathbf{A}(t), \mathbf{B}_f(t), \mathbf{B}_u(t), \boldsymbol{\theta}(t)\}$ , which includes model parameters governing the crowd

dynamics, where  $\mathbf{A}(t)$ ,  $\mathbf{B}_f(t)$ ,  $\mathbf{B}_u(t)$  are coefficient matrices for the state space model in Eq. (1), and  $\boldsymbol{\theta}(t)$  refers to the crowd region parameters. Let  $\hat{\boldsymbol{\theta}}_t^A$  be the estimate based on direct observations, denoted as  $\boldsymbol{\Omega}_A$ , by the UAVs with low resolution parameters, its accuracy can be improved by combing the aggregated information from the UGVs, i.e.  $\hat{\boldsymbol{\theta}}_t^G = \Lambda(\boldsymbol{\Omega}_i)$ ,  $i=1, \dots, M$ , where  $\boldsymbol{\Omega}_i$  is the observation of the  $i^{\text{th}}$  individual agent from UGVs.  $\hat{\boldsymbol{\theta}}_t^G$  is the estimate of  $\boldsymbol{\theta}_t$  from aggregated information of the UGVs and  $\Lambda(\cdot)$  is a link function for aggregation. To compensate the information insufficiency of UAVs,  $\hat{\boldsymbol{\theta}}_t^A$  and  $\hat{\boldsymbol{\theta}}_t^G$  are combined to achieve a better parameter estimation for the crowd dynamics as  $\hat{\boldsymbol{\theta}}_t = w_t \hat{\boldsymbol{\theta}}_t^A + (1-w_t) \hat{\boldsymbol{\theta}}_t^G$ , where  $w_t$  is a weighted scalar in balancing the information. To improve the dynamic modeling of the individuals and/or sub-crowds, UAVs' information can be disaggregated to lower-level of UGVs in compensating their disadvantages of limited observation range. Let  $\boldsymbol{\theta}_{t,i} = \{\mathbf{A}_i(t), \mathbf{B}_{f,i}(t), \mathbf{B}_{u,i}(t)\}$  denote the parameters in characterizing dynamics of the  $i^{\text{th}}$  individual agent, its estimation accuracy can be improved by disaggregating information from the UAVs, i.e.  $\hat{\boldsymbol{\theta}}_{t,i}^A = \Gamma(\boldsymbol{\Omega}_A)$ , where  $\Gamma(\cdot)$  is the disaggregation link function, and be combined with the UGVs' estimate,  $\hat{\boldsymbol{\theta}}_{t,i}^G$ , as  $\hat{\boldsymbol{\theta}}_{t,i} = w_{t,i} \hat{\boldsymbol{\theta}}_{t,i}^A + (1-w_{t,i}) \hat{\boldsymbol{\theta}}_{t,i}^G$ .

Based on the predicted locations of individual agents in the crowd, UGVs need to determine the locations of UGVs at the next time step. Since the objective of UGVs is to control the crowd, the optimal location at the next time step for UGVs is the one that maximizes a given performance indicator. In this paper, coverage probability is considered as the performance indicator, which can be calculated as the mean probability of individual agents being controlled by UGVs. A higher probability indicates better control of the crowd.

#### 4. Preliminary Results

To demonstrate the performance of the proposed approach, a simulation study is conducted. The study considers the tracking and control of a crowd with  $M=10$  individual agents in a certain area. One UAV and three UGVs cooperatively achieve the detection, tracking and control of the crowd. Fig 5(a) gives an illustration of the scenario, where the dots represent ten individual agents. The shaded region shows that these ten agents form a small crowd and the arrow indicates that these ten agents move together to the right. The red and green circles surrounding a UGV indicate its detection range (subject to sensor device capability and environmental factors) and controllable range (subject to control device capability and environmental factors), respectively. Two parameters, detection radius  $R_d$  and control radius  $R_c$ ,  $R_d > R_c$ , are defined accordingly. The detection radius is used to calculate a detection probability. The control radius, as well as the triangle region formed by connecting the three UGVs, is used to calculate a coverage probability.

$$\begin{bmatrix} x_i(t+1) \\ y_i(t+1) \\ v_{x,i}(t+1) \\ v_{y,i}(t+1) \end{bmatrix} = \begin{bmatrix} 1 & 0 & dt & 0 \\ 0 & 1 & 0 & dt \\ 0 & 0 & 1 & 0 \\ 0 & 0 & 0 & 1 \end{bmatrix} \begin{bmatrix} x_i(t) \\ y_i(t) \\ v_{x,i}(t) \\ v_{y,i}(t) \end{bmatrix} + \begin{bmatrix} e_{x,i}(t) \\ e_{y,i}(t) \\ e_{vx,i}(t) \\ e_{vy,i}(t) \end{bmatrix} \text{ and } \begin{bmatrix} \tilde{x}_i(t) \\ \tilde{y}_i(t) \end{bmatrix} = \begin{bmatrix} 1 & 0 & 0 & 0 \\ 0 & 1 & 0 & 0 \end{bmatrix} \begin{bmatrix} x_i(t) \\ y_i(t) \\ v_{x,i}(t) \\ v_{y,i}(t) \end{bmatrix} + \begin{bmatrix} \varepsilon_{x,i}(t) \\ \varepsilon_{y,i}(t) \end{bmatrix} \quad (2)$$

In the simulation study, the initial locations of the individual agents are randomly generated from a bivariate normal distribution with mean (0,0) and diagonal variance matrix being 0.01, with proper unit. The dynamics of the individual agents are specified through the assumed state space model, shown in Eq. (2), where  $v_{x,i}(t) = 0.15$  and  $v_{y,i}(t) = 0$ ,  $i=1,2, \dots, M$ . The noises of locations and speed along x-axis and y-axis follow normal distribution with mean 0 and variance 0.01. Individual agents move to the right with location and speed impacted by additive Gaussian noise. To simplify this study, the environmental factors and control factors are not considered.

Due to the measurement accuracy of the sensors onboard the UGV, the observation model in Eq. (2) is used to link the true state of the individual agents, and the observations  $[\tilde{x}_i(t), \tilde{y}_i(t)]$  show that the detected area are formed with true state plus the additive Gaussian noise with mean 0 and variance  $0.05^2$ .

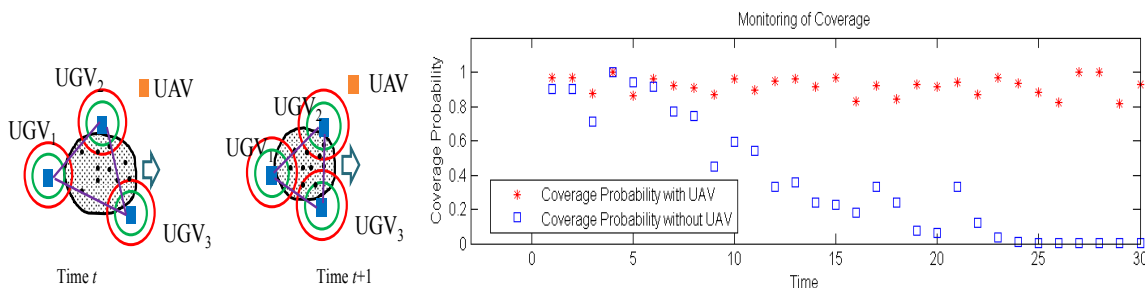


Figure 5. (a) Illustration of simulated scenario; (b) Coverage probability of exemplary simulation run

As aforementioned, the individual agents may not be detected all the time. The UGVs detect them with a probability, which is a function of distance and parameter  $R_d$ . In the study, this probability is specified as  $Pr(\text{detection})=2(1-\Phi(d/R_d))$ , where  $d$  denotes the distance,  $\Phi$  is the cumulative distribution function of standard normal distribution and detection radius  $R_d$ ,  $R_d = 1.5$ , is used to quantify the detection capability. Larger  $R_d$  indicates that when a distance between the UGV and individual agent is fixed, the UGV has a higher detection probability.

To improve the UGV’s performance in tracking and controlling individual agents, the study assumes that information disaggregation from UAV can improve the detection and control capability of UGVs. Specifically, the detection radius and control radius of UGVs, with UAVs’ disaggregated information, is three times as large as that without. The increased detection and control radius will improve tracking and control performance.

The predicted individual locations from Kalman filter are sent to UGVs so that path planning can be performed. The study considers a simplified planning scenario where each UGV can either stop (i.e. staying in the center of the three by three grids) or move to one of the eight neighboring grids. The combination of candidate locations from all the three UGVs constitutes the search space for the optimal plan. Such a combination of locations will be assigned to the UGVs at the next time step. The coverage probability is defined as a function of UGV locations, predicted locations of individual agents, and a parameter  $R_c$  specifying the control capability of UGV. As shown in Fig 5(a), for individual agents beyond the triangle formed by UGVs, their probability of being controlled by a UGV in a distance  $d$  is given as  $Pr(\text{control})=2(1-\Phi(d/R_c))$ , with  $R_c=1.2$ . When the individual agent is within the triangle, the control probability is tripled. The overall coverage probability of the whole crowd is the mean coverage probability of individual agents.

The simulation experiment is conducted 100 replications to compare the performance in two scenarios, one is with the information disaggregated from UAV (denoted as “with UAV”) and the other is without information from UAVs (denoted as “without UAV”). In each replication, the simulation runs for 30 time steps, and the mean coverage probability at each time step is calculated. In the simulation run, the coverage probability at each time step is calculated and visualized, as shown in Fig 5(b). The horizontal axis represents the time and has 30 points in total for the whole simulation run. The vertical axis shows the coverage probability for two scenarios. The two curves in the figure begin to diverge at about 7<sup>th</sup> time units. This divergence represents the case that UGVs gradually lose control of the crowd due to limited detection and control capability.

The collected mean coverage probabilities  $P_c$  from 100 replications under the two settings are compared via hypothesis testing. Table 1 summarizes the mean of  $P_c$  and sample standard deviation in 100 replications. A

test on the equal-variance is firstly conducted and it rejects the equal-variance hypothesis. Then, hypothesis test on mean  $P_c$  with unequal variance assumption indicates the significant performance improvement in crowd control when UGVs receive disaggregated information from UAV.

Table 1. Summary of 100 replications

	Sample mean of $P_c$	Sample standard deviation of $P_c$
Without UAV	0.6126	0.1606
With UAV	0.9099	0.0337

## 5. Conclusions and Future Research

A DDDAMS-based planning and control framework has been proposed for crowd control via UAVs and UGVs. Models and algorithms have been also proposed for crowd motion detection, tracking, and control. The simulation study has demonstrated the benefits of the proposed algorithms (e.g. information disaggregation) on the performance improvement of crowd surveillance. It is noted that  $M$ , the number of individual agents may significantly affect the performance of crowd tracking and control. One limitation of the current work is that it assumes UAVs provide enhancement in detecting each individual agent in the crowd. There can be scenarios that UAV may not be able to observe on individual scales. Instead, UAV observes only the dense region of a crowd. Information aggregation/disaggregation under this scenario will be considered as a future work.

## Acknowledgements

This work was supported by the Air Force Office of Scientific Research under FA9550-12-1-0238.

## References

- [1] Celik, N., S. Lee, K. Vasudevan, and Y. Son (2010). "DDDAS-based Multi-fidelity Simulation Framework for Supply Chain Systems." *IEEE Transactions on Operations Engineering* 42(5): 325-341.
- [2] Grocholsky, B., et al., Cooperative air and ground surveillance. *Robotics & Automation Magazine*, IEEE, 2006. 13(3): p. 16-25.
- [3] De Filippis, L. and G. Guglieri, Path Planning strategies for UAVs in 3D environments. *Journal of Intelligent & Robotic Systems* 65.1 (2012): 247-264.
- [4] Evsen et al. On path planning strategies for networked unmanned aerial vehicles. *Computer Communications Workshops (INFOCOM WKSHPS)*, 2011 IEEE Conference on 10 Apr. 2011: 212-216.
- [5] Welch, G. and G. Bishop, An introduction to the Kalman filter. 1995.
- [6] C. Becker, H. González-Baños, J.-C. Latombe, and C. Tomasi, "An Intelligent Observer," in *The 4th International Symposium on Experimental Robotics IV*, 1997, pp. 153–160.
- [7] T. Oskam, R. W. Sumner, N. Thuerey, and M. Gross, "Visibility transition planning for dynamic camera control," in *SCA '09: Proceedings of the 2009 ACM SIGGRAPH/Eurographics Symposium on Computer Animation*, 2009, pp. 55–65.
- [8] C. Vo, S. McKay, N. Garg, and J.-M. Lien, "CIO: Cached Intelligent Observer," in *Motion in Game*, 2012.
- [9] Pavlovic, V., J.M. Rehg, and J. MacCormick, Learning switching linear models of human motion. *Advances in Neural Information Processing Systems*, 2001: p. 981-987.
- [10] Arulampalam, M.S., et al., A tutorial on particle filters for online nonlinear/non-Gaussian Bayesian tracking. *Signal Processing, IEEE Transactions on*, 2002. 50(2): p. 174-188.
- [11] Silbert, M., T. Mazzuchi, and S. Sarkani. Comparison of a grid-based filter to a Kalman filter for the state estimation of a maneuvering target. in *Society of Photo-Optical Instrumentation Engineers (SPIE) Conference Series*. 2011.
- [12] Ristic, B., S. Arulampalam, and N. Gordon, *Beyond the Kalman filter: Particle filters for tracking applications*. 2004: Artech House Publishers.